

Insight into the Natural Convection Flow Through a Vertical Cylinder Using Caputo Time-Fractional Derivatives

Nehad Ali Shah¹ · Thanaa Elnaqeeb² ·
I. L. Animasaun³  · Yasir Mahsud¹

Published online: 12 April 2018
© Springer (India) Private Ltd., part of Springer Nature 2018

Abstract The variation in temperature distribution with time for the case of the fractional model which models the flow of fluid through a vertical cylinder is considered. This article provides an insight into the natural convective flow of a viscous fluid through a vertical heated cylinder using the fractional differential equation with Caputo derivatives. Analytical solutions for temperature and velocity functions were obtained using Laplace transform and finite Hankel integral transform methods. Stehfest's algorithm was used to obtain the inverse Laplace transforms. Numerical simulations and graphical illustrations were carried out in order to analyze the influence of the time-fractional derivative on the transport phenomenon. The significant difference between the fractional fluid flow and ordinary fluid at various time (t) is unraveled. At the initial time, the flow of fractional fluid is faster than the ordinary fluid.

Keywords Natural convection flow · Vertical cylinder · Laplace and finite Hankel transforms · Caputo time-fractional derivative

✉ I. L. Animasaun
anizakph2007@gmail.com

Nehad Ali Shah
nehadali199@yahoo.com

Thanaa Elnaqeeb
thanaa_1@yahoo.com

Yasir Mahsud
yasirmahsud16@gmail.com

¹ Abdus Salam School of Mathematical Sciences, GC University Lahore, Lahore, Pakistan

² Department of Mathematics, Faculty of Science, Zagazig University, Zagazig 44519, Egypt

³ Department of Mathematical Sciences, Federal University of Technology, Akure, Nigeria

Introduction

It is worth noticing within the last few decades that a considerable attention has been devoted to exploring the heat and/or mass transfer in the flow of various fluids over cylindrical domains. Considering the relevance of cyclones in the industry, Zhao and Abrahamson [1] stated that the body of this kind of object may be either conical or cylindrical, or made of both geometries. Thereafter, heat transfer through cylindrical objects (i.e. domains) has been pointed out in building machines, materials processing, solar collectors, furnace designs, heat exchangers, storage tanks, and nuclear designs. Sharma et al. [2], Franke and Hutson [3], Roschina et al. [4] and Bairi [5] investigated the convection heat transfer in cylindrical domains by assuming that the density varies according to Boussinesq approximation and the other thermo-physical fluid properties are constant. In Ref. [2] it is revealed that the intensity of heat source decays exponentially with time and concluded in Ref. [3] that increase in heat transfer is based on the heat input required to maintain the inside surface of the cylinder at a constant temperature. According to the report of Morgan [6] in the year 1975 on the natural convection from smooth circular cylinders, it is also revealed that there is a wide dispersion in the results of experiments due to axial heat conduction losses to the supporting structures of the horizontal cylinders and velocity fields by convective fluid movements. Moreover, Lemembre and Petit [7] introduced a numerical investigation of heat transfer of the two-dimensional natural convection laminar flow in cylindrical enclosures of heated lateral walls at uniform heat flux and cooled at the same heat flux at the top surface by insulating the bottom surface. The steady natural convection laminar flow in rectangular domains has been presented by Chen and Humphrey [8]. Kim and Viskanta [9], and Vargas et al. [10] introduced both experimental and numerical investigations to discuss the natural convection steady flow in two-dimensional Newtonian and incompressible fluid-filled enclosures. Makinde and Animasaun [11, 12], Animasaun [13] and Koriko et al. [14] discussed three convection fluid flow modes within the boundary layer. In addition, experimental and numerical investigations have been introduced by Kee et al. [15] for steady flow natural convection of heat generating tritium gas in two-dimensional closed vertical cylinders and spheres with their bounding isothermal walls. For more reports on free convection flow of Cattaneo–Christov fluid, axisymmetric Powell–Eyring fluid, Jeffrey nanofluid, micropolar flow using a modified Boussinesq approximation, and unsteady mixed convection MHD; see Refs. [16–23].

An experiment has been performed by Bohn and Anderson [24] to study the model of heat transfer of natural convection flow between both perpendicular and parallel vertical walls. They considered three-dimensional cubic enclosure filled with water. Moreover, they assumed that the cubic enclosure has isothermal sides and adiabatic top and bottom. The two-dimensional conjugate natural convection laminar flow in an enclosure was introduced numerically by Liaqat and Baytas [25]. In addition, Kuznetsov and Sheremet [26] investigated numerically the two-dimensional conjugate convective-conductive heat transfer in a rectangular enclosure due to the local heat and contaminant sources. Fractional calculus can provide a concise model for the description of the dynamic events. Such a description is important for gaining an understanding of the underlying multiscale processes. The mathematics of fractional calculus has been applied successfully in physics, chemistry, and materials science to describe dielectrics, electrodes and viscoelastic materials over extended ranges of time and frequency. In heat and mass transfer, for example, the half-order fractional integral is the natural mathematical connection between thermal or material gradients and the diffusion of heat or ions. Therefore fractional calculus is being applied to build new mathematical models. Suitable information on viscoelastic properties of polymer and elastomers is necessary for an accurate modeling and analysis of structures with dynamic and vibration problems.

When experimental data is used to correlate with the fractional order model results, it shows good agreement and has the capability to reproduce the experimental data for given material; see Sasso et al. [27]. Viscoelastic models based on the noninteger order calculus was introduced by Sloninsky [28]. The mechanical responses predicted by such models were found to be consistent with the molecular theory of polymers by Bagley and Torvik [29]. Schiessel and Blumen [30] derived mechanical analogs to fractional derivative elements and models by assembling numerous springs and dashpots (elastic and viscous terms, respectively) in series and parallel. The fractional models of increasing complexity were proposed by Song and Jiang [31] to simulate the rheological behavior of synthetic polymers as well as biological cells and tissues see Djordjevic et al. [32], Heymans [33], and Liu et al. [34]. For more details about mathematical models for fractional derivatives applications; see Chatterjee [35], Pfitzenreiter [36], and Kawada [37]. Finally, the review of the literature reveals that natural convective flow with heat transfer of a viscous fluid through a vertical cylinder using fractional equations with Caputo derivatives is still an open question, hence this study.

Problem Formulation

In this report, unsteady, laminar and incompressible viscous flows through an infinite vertical cylinder of the radius are considered. Here, the z -axis is taken along the axis of the cylinder in the vertically upward direction, and the radial coordinate r is taken normal to it. Initially, it is assumed that the cylinder and the fluid are at the same temperature T_∞ and the concentration on cylinder surface is C_∞ .

At time $t > 0$, the temperature and concentration on the cylinder surface are raised to T_w and C_w , respectively (see Fig. 1). Following Deka et al. [38] and using Boussinesq’s approximation, the governing equation is of the form

$$\frac{\partial^2 u}{\partial r^2} + \frac{1}{r} \frac{\partial u}{\partial r} + \frac{g\beta_T}{\nu}(T - T_\infty) + \frac{g\beta_C}{\nu}(C - C_\infty) = \frac{1}{\nu} \frac{\partial u}{\partial t}; \quad r \in (0, r_0), \quad t > 0, \quad (1)$$

$$\frac{\partial^2 T}{\partial r^2} + \frac{1}{r} \frac{\partial T}{\partial r} - \frac{1}{\alpha_0} \frac{\partial T}{\partial t} = 0; \quad r \in (0, r_0), \quad t > 0, \quad (2)$$

$$\frac{\partial^2 C}{\partial r^2} + \frac{1}{r} \frac{\partial C}{\partial r} - \frac{1}{D} \frac{\partial C}{\partial t} = 0; \quad r \in (0, r_0), \quad t > 0, \quad (3)$$

The appropriate initial and boundary conditions are:

$$\begin{aligned} u = 0, \quad T = T_\infty, \quad C = C_\infty; \quad r \in [0, r_0], \quad t = 0, \\ u = 0, \quad T = T_w, \quad C = C_w; \quad r = r_0, \quad t > 0. \end{aligned} \quad (4)$$

where α_0 is the thermal diffusivity and D is the mass diffusivity coefficient. Introducing the following dimensionless variables:

$$\begin{aligned} t^* = \frac{t\nu}{r_0^2}, \quad r^* = \frac{r}{r_0}, \quad u^* = \frac{ur_0}{\nu}, \quad T^* = \frac{T - T_\infty}{T_w - T_\infty}, \quad C^* = \frac{C - C_\infty}{C_w - C_\infty}, \quad \text{Pr} = \frac{\nu}{\alpha_0}, \quad \text{Sc} = \frac{\nu}{D}, \\ Gr = \frac{g\beta_T(T_w - T_\infty)r_0^3}{\nu^2}, \quad Gm = \frac{g\beta_C(C_w - C_\infty)r_0^3}{\nu^2}, \end{aligned} \quad (5)$$

where Pr is the Prandtl number, Sc is the Schmidt number, Gr is the thermal Grashof number and Gm is the solutal Grashof number. The governing Eqs. (1)–(4) reduce to

$$\frac{\partial u(r, t)}{\partial t} = \frac{\partial^2 u(r, t)}{\partial r^2} + \frac{1}{r} \frac{\partial u(r, t)}{\partial r} + GrT(r, t) + GmC(r, t); \quad r \in (0, 1), \quad t > 0, \quad (6)$$

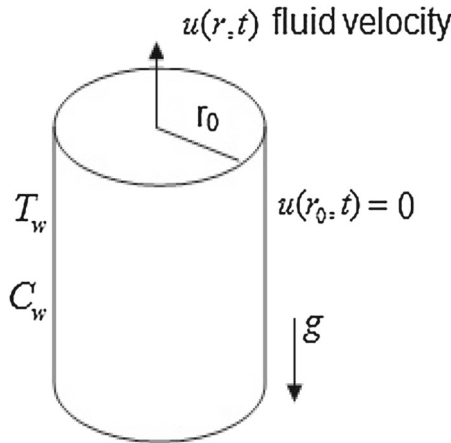


Fig. 1 The physical model

$$\frac{\partial T(r, t)}{\partial t} = \frac{1}{Pr} \left(\frac{\partial^2 T(r, t)}{\partial r^2} + \frac{1}{r} \frac{\partial T(r, t)}{\partial r} \right); \quad r \in (0, 1), t > 0, \tag{7}$$

$$\frac{\partial C(r, t)}{\partial t} = \frac{1}{Sc} \left(\frac{\partial^2 C(r, t)}{\partial r^2} + \frac{1}{r} \frac{\partial C(r, t)}{\partial r} \right); \quad r \in (0, 1), \quad t > 0, \tag{8}$$

$$u(r, 0) = 0, \quad T(r, 0) = 0, \quad C(r, 0) = 0; \quad r \in [0, 1], \tag{9}$$

$$u(1, t) = 0; \quad T(1, t) = 1, \quad C(1, t) = 1, \quad t > 0. \tag{10}$$

In order to develop a fractional model following Lorenzo and Hartley [39], the ordinary time-derivative is replaced with Caputo derivative of fractional order α for $0 < \alpha < 1$. This leads to

$$D_t^\alpha u(r, t) = \frac{\partial^2 u(r, t)}{\partial r^2} + \frac{1}{r} \frac{\partial u(r, t)}{\partial r} + GrT(r, t) + GmC(r, t); \quad r \in (0, 1), \quad t > 0, \tag{11}$$

$$D_t^\alpha T(r, t) = \frac{1}{Pr} \left(\frac{\partial^2 T(r, t)}{\partial r^2} + \frac{1}{r} \frac{\partial T(r, t)}{\partial r} \right); \quad r \in (0, 1), \quad t > 0, \tag{12}$$

$$D_t^\alpha C(r, t) = \frac{1}{Sc} \left(\frac{\partial^2 C(r, t)}{\partial r^2} + \frac{1}{r} \frac{\partial C(r, t)}{\partial r} \right); \quad r \in (0, 1), \quad t > 0, \tag{13}$$

where $D_t^\alpha u(y, t)$ —the Caputo derivative of fractional order of the function $u(r, t)$ is given as:

$$D_t^\alpha u(r, t) = \begin{cases} \frac{1}{\Gamma(1-\alpha)} \int_0^t \frac{u'(r, \tau)}{(t-\tau)^\alpha} d\tau & 0 \leq \alpha < 1 \\ u'(r, t), & \alpha = 1 \end{cases}, \tag{14}$$

where $\Gamma(\cdot)$ is the Gamma function.

Method of Solution

Applying the Laplace transform to Eq. (12) and using the initial and boundary conditions Eqs. (9) and (10), leads to the following transformed problem:

$$q^\alpha \bar{T}(r, q) = \frac{1}{Pr} \left(\frac{\partial^2}{\partial r^2} + \frac{1}{r} \frac{\partial}{\partial r} \right) \bar{T}(r, q), \tag{15}$$

$$\bar{T}(1, q) = \frac{1}{q}, \tag{16}$$

where $\bar{T}(r, q)$ is the Laplace transform of the function $T(r, t)$ and q is the transform variable. Applying the finite Hankel transform of order zero to Eq. (15) and using condition Eq. (16). This leads to

$$\bar{T}_H(r_n, q) = \frac{r_n J_1(r_n)}{Pr} \frac{1}{q \left(q^\alpha + \frac{r_n^2}{Pr} \right)}, \tag{17}$$

where $\bar{T}_H(r_n, q) = \int_0^1 r \bar{T}(r, q) J_0(rr_n) dr$ is the finite Hankel transform of the function $\bar{T}(r, q)$, $r_n, n = 0, 1, \dots$ are the positive roots of the equation $J_0(x) = 0$, J_0 being the Bessel function of first kind and zero order. Equation (17) can be written in the equivalent form as

$$\bar{T}(r_n, q) = \frac{J_1(r_n)}{r_n} \frac{1}{q} - \frac{J_1(r_n)}{r_n} \frac{q^{\alpha-1}}{q^\alpha + \frac{r_n^2}{Pr}}. \tag{18}$$

Taking the inverse Laplace transform of Eq. (18), leads to

$$T_H(r_n, t) = \frac{J_1(r_n)}{r_n} - \frac{J_1(r_n)}{r_n} R_{\alpha, \alpha-1} \left(t, -\frac{r_n^2}{Pr} \right), \tag{19}$$

where $R_{\sigma, \nu}(t, a) = L^{-1} \left\{ \frac{q^\nu}{q^\sigma - a} \right\} = \sum_{m=0}^\infty \frac{a^m t^{(m+1)\sigma - \nu - 1}}{\Gamma[(m+1)\sigma - \nu]}$; $\text{Re}(\sigma - \nu) > 0$, is the Lorenzo-Hartley’s function [38]. Taking the inverse Hankel transform. Leads to

$$T(r, t) = 1 - 2 \sum_{n=1}^\infty \frac{J_0(rr_n)}{r_n J_1(r_n)} R_{\alpha, \alpha-1} \left(t, -\frac{r_n^2}{Pr} \right); \quad 0 < \alpha < 1. \tag{20}$$

For the case when $\alpha = 1$, easy to deduce that $R_{1,0} \left(t, -\frac{r_n^2}{Pr} \right) = \exp \left(-\frac{r_n^2}{Pr} t \right)$, so the temperature profile become

$$T(r, t) = 1 - 2 \sum_{n=1}^\infty \frac{J_0(rr_n)}{r_n J_1(r_n)} \exp \left(-\frac{r_n^2}{Pr} t \right); \quad \alpha = 1. \tag{21}$$

In the same line as the temperature distribution, the species concentration is obtained as

$$C(r, t) = 1 - 2 \sum_{n=1}^\infty \frac{J_0(rr_n)}{r_n J_1(r_n)} R_{\alpha, \alpha-1} \left(t, -\frac{r_n^2}{Sc} \right); \quad 0 < \alpha < 1, \tag{22}$$

$$C(r, t) = 1 - 2 \sum_{n=1}^\infty \frac{J_0(rr_n)}{r_n J_1(r_n)} \exp \left(-\frac{r_n^2}{Sc} t \right); \quad \alpha = 1, \tag{23}$$

with Laplace and finite Hankel transform

$$\bar{C}_H(r_n, q) = \frac{r_n J_1(r_n)}{Sc} \frac{1}{q \left(q^\alpha + \frac{r_n^2}{Sc} \right)}, \tag{24}$$

that will be used to obtaining the velocity field. Applying the Laplace transform to Eq. (11), using the initial and boundary conditions (9) and (10), leads to

$$q^\alpha \bar{u}(r, q) = \frac{\partial^2 \bar{u}(r, q)}{\partial r^2} + \frac{1}{r} \frac{\partial \bar{u}(r, q)}{\partial r} + Gr \bar{T}(r, q) + Gm \bar{C}(r, q), \tag{25}$$

$$\bar{u}(1, q) = 0. \tag{26}$$

Applying finite Hankel transform to Eq. (25), using boundary condition (26) and Eqs. (17), (24), leads to

$$\bar{u}_H(r_n, q) = \frac{Gr}{Pr} \frac{r_n J_1(r_n)}{q \left(q^\alpha + \frac{r_n^2}{Pr} \right) \left(q^\alpha + r_n^2 \right)} + \frac{Gm}{Sc} \frac{r_n J_1(r_n)}{q \left(q^\alpha + \frac{r_n^2}{Sc} \right) \left(q^\alpha + r_n^2 \right)}, \tag{27}$$

where $\bar{u}_H(r_n, q) = \int_0^1 r \bar{u}_H(r, q) J_0(rr_n) dr$ is the finite Hankel transform of the function $\bar{u}(r, q)$.

Equation (27), can be written in the following equivalent form

$$\bar{u}_H(r_n, q) = \frac{N J_1(r_n)}{r_n} \frac{1}{q \left(q^\alpha + r_n^2 \right)} - \frac{Gr J_1(r_n)}{r_n} \frac{q^{\alpha-1}}{\left(q^\alpha + \frac{r_n^2}{Pr} \right) \left(q^\alpha + r_n^2 \right)} - \frac{Gm J_1(r_n)}{r_n} \frac{q^{\alpha-1}}{\left(q^\alpha + \frac{r_n^2}{Sc} \right) \left(q^\alpha + r_n^2 \right)}, \tag{28}$$

where $N = Gr + Gm$.

Taking inverse Laplace transform of the Eq. (28), leads to

$$u_H(r_n, q) = \frac{N J_1(r_n)}{r_n} H(t) * F_\alpha(t, -r_n^2) - \frac{Gr J_1(r_n)}{r_n} R_{\alpha, \alpha-1} \left(t, -\frac{r_n^2}{Pr} \right) * F_\alpha(t, -r_n^2) - \frac{Gm J_1(r_n)}{r_n} R_{\alpha, \alpha-1} \left(t, -\frac{r_n^2}{Sc} \right) * F_\alpha(t, -r_n^2), \tag{29}$$

where $H(t)$ is Heaviside unit step function, $L^{-1} \left\{ \frac{1}{q^\alpha + b} \right\} = F_\alpha(-b, t) = \sum_{n=0}^\infty \frac{(-b)^n t^{(n+1)\alpha-1}}{\Gamma[(n+1)\alpha]}$ is the Robrtnov and Hartley’s function Ref. [38] and “*” represents the convolution product. Inverting the Hankel transform leads to

$$u(r, t) = 2 \sum_{n=1}^\infty \frac{J_0(rr_n)}{J_1^2(r_n)} u_H(r_n, t), \\ = 2 \sum_{n=1}^\infty \frac{J_0(rr_n)}{r_n J_1(r_n)} \left[\begin{aligned} &N H(t) * F(t, -r_n^2) - Gr R_{\alpha, \alpha-1} \left(t, -\frac{r_n^2}{Pr} \right) * F(t, -r_n^2) \\ &- Gm R_{\alpha, \alpha-1} \left(t, -\frac{r_n^2}{Sc} \right) * F(t, -r_n^2), \end{aligned} \right]. \tag{30}$$

In the case $\alpha = 1$, $F_1(t, -a_0) = R_{1,0}(t, -a_0) = e^{-a_0 t}$.

Semi-analytical Solution

Given that the velocity expression Eq. (30) is complicated, therefore, difficult to use in numerical calculations, in this section a semi-analytical solution for the velocity field is

presented. It is observed that, the temperature and concentration are solutions of the partial differential equation

$$k_0 D_t^\alpha w(r, t) = \frac{\partial^2 w(r, t)}{\partial r^2} + \frac{1}{r} \frac{\partial w(r, t)}{\partial r}, \tag{31}$$

along with the initial and boundary conditions

$$w(r, 0) = 0, \quad w(1, t) = 1. \tag{32}$$

The temperature and concentration solutions are corresponding to $k_0 = Pr$, and $k_0 = Sc$, respectively. By applying the Laplace transform with respect to t to Eq. (31), the transformed problem can be written in the equivalent form:

$$r^2 \bar{w}''(r, q) + r \bar{w}'(r, q) - \left(r\sqrt{k_0 q^\alpha}\right)^2 \bar{w}(r, q) = 0, \tag{33}$$

$$\bar{w}(1, q) = \frac{1}{q}. \tag{34}$$

Equation (33) is a modified Bessel equation with the general solution (bounded for $r \in [0, 1]$)

$$\bar{w}(r, q) = C_1 I_0 \left(r\sqrt{k_0 q^\alpha}\right),$$

where $I_0(\cdot)$ is the modified Bessel function of first kind and order zero. Using the boundary condition (34), the solution of Eqs. (33)–(34) is of the form

$$\bar{w}(r, q) = \frac{1}{q} \frac{I_0 \left(r\sqrt{k_0 q^\alpha}\right)}{I_0 \left(\sqrt{k_0 q^\alpha}\right)}. \tag{35}$$

Now, using Eq. (35) into Eq. (25) the transform problem of the velocity function is of the form

$$q^\alpha \bar{u}(r, q) = \frac{\partial^2 \bar{u}(r, q)}{\partial r^2} + \frac{1}{r} \frac{\partial \bar{u}(r, q)}{\partial r} + \frac{Gr}{q} \frac{I_0 \left(r\sqrt{Pr q^\alpha}\right)}{I_0 \left(\sqrt{Pr q^\alpha}\right)} + \frac{Gm}{q} \frac{I_0 \left(r\sqrt{Sc q^\alpha}\right)}{I_0 \left(\sqrt{Sc q^\alpha}\right)}, \tag{36}$$

$$\bar{u}(1, q) = 0. \tag{37}$$

A particular solution of Eq. (36) is

$$\bar{u}_p(r, q) = \frac{Gr}{1 - Pr} \frac{I_0 \left(r\sqrt{Pr q^\alpha}\right)}{q^{\alpha+1} I_0 \left(\sqrt{Pr q^\alpha}\right)} + \frac{Gm}{1 - Sc} \frac{I_0 \left(r\sqrt{Sc q^\alpha}\right)}{q^{\alpha+1} I_0 \left(\sqrt{Sc q^\alpha}\right)}, \quad Pr \neq 1, \quad Sc \neq 1, \tag{38}$$

The general solution bounded for $r \in [0, 1]$ is

$$\bar{u}(r, q) = C_2 I_0 \left(r\sqrt{q^\alpha}\right) + \bar{u}_p(r, q). \tag{39}$$

By using the boundary condition Eq. (37), the Laplace transform of the velocity field is of the form

$$\bar{u}(r, q) = \frac{1}{q^{\alpha+1}} \left[\frac{Gr}{1 - Pr} \frac{I_0 \left(r\sqrt{Pr q^\alpha}\right)}{I_0 \left(\sqrt{Pr q^\alpha}\right)} + \frac{Gm}{1 - Sc} \frac{I_0 \left(r\sqrt{Sc q^\alpha}\right)}{I_0 \left(\sqrt{Sc q^\alpha}\right)} - \left(\frac{Gr}{1 - Pr} + \frac{Gm}{1 - Sc} \right) \frac{I_0 \left(r\sqrt{q^\alpha}\right)}{I_0 \left(\sqrt{q^\alpha}\right)} \right]. \tag{40}$$

Even if the analytical form of the inverse Laplace transform of function $\bar{u}(r, q)$ can be obtained (using the residue theorem, for example), in this study the Stehfest’s algorithm Refs. [40–42]

Table 1 Numerical values of the Eqs. (30) and (41) at $\alpha = 0.5, Pr = 2, Sc = 1.5, Gr = 1.4$ and $Gm = 2.5$ for different values of time t

r	t=0.2		t=0.3		t=0.8	
	Eq. (30)	Eq. (41)	Eq. (30)	Eq. (41)	Eq. (30)	Eq. (41)
0	0.48436	0.48458	0.63626	0.63648	0.70269	0.70271
0.1	0.48111	0.48131	0.63108	0.63127	0.69666	0.69664
0.2	0.47114	0.47132	0.61539	0.61552	0.67843	0.67832
0.3	0.45394	0.45407	0.58879	0.5888	0.64765	0.64741
0.4	0.42857	0.42862	0.55058	0.55043	0.60373	0.60333
0.5	0.39372	0.39367	0.49975	0.49943	0.54584	0.54527
0.6	0.34767	0.34748	0.43502	0.43454	0.4729	0.47213
0.7	0.28821	0.2879	0.35476	0.35418	0.38355	0.38277
0.8	0.21267	0.2123	0.25705	0.25649	0.2762	0.27551
0.9	0.11792	0.11755	0.13963	0.13927	0.14902	0.1486
1	0	0	0	0	0	0

is adopted for numerical inversion of the Laplace transform, namely, the velocity field $u(r, t)$ is approximated by

$$u(r, t) \approx \frac{\ln(2)}{t} \sum_{j=1}^{2p} k_j \bar{u} \left(r, j \frac{\ln(2)}{t} \right), \tag{41}$$

where $k_j = (-1)^{j+p} \sum_{i=\lfloor \frac{j+1}{2} \rfloor}^{\min(j,p)} \frac{i^p (2i)!}{(p-i)! i! (i-1)! (j-i)! (2i-j)!}$, p is a positive integer number, $\lfloor \frac{j+1}{2} \rfloor$

is the integer part of the real number $\frac{j+1}{2}$ and $\min(j, p) = \frac{1}{2} [i + j - |i - j|]$. In order to verify the numerical results, the values obtaining with Eqs. (30) and (41) are presented in Table 1. It is observed that there is a good agreement between results obtained with both formulas. Also, the absolute errors for different numbers of terms in the series solution are given in Table 2.

Numerical Results and Discussion

In this paper we have studied convective flows of the unsteady, laminar and incompressible viscous flow through an infinite vertical cylinder with constant temperature and concentration on the surface. The fluid temperature, concentration and velocity fields are obtained as solutions of the fractional differential equations with time-fractional derivatives of Caputo type. Numerical results obtained with the software Mathcad are presented in graphical illustrations. Especially, we studied the influence of the fractional parameter α on the fluid temperature and velocity to compare it with the ordinary case $\alpha = 1$. In Figs. 2 and 3, the graphs of dimensionless temperature versus r , for the variation of fractional parameter α , and consider the different values of time t are illustrated. Form Fig. 2, it is clear that the temperature of the fluid is decreases by increasing the value of α . But the temperature of the fluid is increasing with increasing time t and the temperature difference is decrease and we consider this is a small time. Figure 3 is sketch to study the effect of fractional parameter α , for larger values of

Table 2 Absolute errors for values of velocity given by Eqs. (30) and (41)

r	n = 100			n = 1000		
	Eq. (30)	Eq. (41)	Eqs. (30)–(41)	Eq. (30)	Eq. (41)	Eqs. (30)–(41)
0	0.63626	0.63648	2.188×10^{-4}	0.63626	0.63648	2.16×10^{-4}
0.1	0.63108	0.63127	1.928×10^{-4}	0.63108	0.63127	1.925×10^{-4}
0.2	0.61539	0.61552	1.225×10^{-4}	0.61539	0.61552	1.223×10^{-4}
0.3	0.58879	0.5888	8.263×10^{-6}	0.58879	0.5888	8.039×10^{-6}
0.4	0.55053	0.55043	1.433×10^{-4}	0.55058	0.55043	1.436×10^{-4}
0.5	0.49975	0.49943	3.154×10^{-4}	0.49975	0.49943	3.157×10^{-4}
0.6	0.43502	0.43454	4.782×10^{-4}	0.43502	0.43454	4.784×10^{-4}
0.7	0.35476	0.35418	5.823×10^{-4}	0.35476	0.35418	5.826×10^{-4}
0.8	0.25705	0.25649	5.634×10^{-4}	0.25705	0.25649	5.638×10^{-4}
0.9	0.13963	0.13927	3.638×10^{-4}	0.13963	0.13927	3.646×10^{-4}
1	0	0	0	0	0	0

the time t . In this case, the fluid temperature decreases if the fractional parameter decreases. Note that, for small values of the time t the heat transfer decreases at small values of the fractional parameter, but, the heat transfer increases at larger values of the time t and decreasing values of the fractional parameter. These aspects are well highlighted by the curves plotted in Fig. 4. The effect of Prandtl number Pr , on dimensionless temperature, for different values of time t is graphically studied in Fig. 5. As expected, for increasing values of the Prandtl number the temperature decreases, because, for large values of Prandtl number, the momentum diffusivity dominates so, the thermal diffusivity is small. The influence of the fractional parameter on the fluid velocity was analyzed in Figs. 6, 7 and 8. At small values of the time t , the velocity of fluids modeled by fractional derivatives is bigger than velocity of ordinary fluid. At larger values of the time t , the fractional fluids flow slower than the ordinary fluid. Comparing the numerical values of velocity, obtained with both solutions, it is found a good agreement (see Table 1). In order to analyze the influence of the time-fractional derivative on the fluid flow parameter, numerical results are extracted from the analytical expressions and are illustrated through graphs. It is found that fluids modeled with the fractional differential equations, behave differently from ordinary fluids. At large values of time, the fractional fluid model flows slower than the ordinary fluid model, while at small values of time, the fractional fluid model flows faster than the ordinary fluid model.

Conclusion

In this paper we studied the convective flow with heat and mass transfer of a viscous fluid modeled by fractional differential equations with Caputo derivatives, through a vertical cylinder. Closed forms of the analytical solutions for temperature, concentration and velocity fields are obtained using the Laplace transform and finite Hankel transform. These solutions are expressed by the generalized functions R-Lorenzo–Hartley functions and T-Robotnov’s functions. Semi-analytical solutions were obtained by coupling the Laplace transform with Bessel equation. For semi-analytical solutions, the inverse Laplace transform was obtained by the

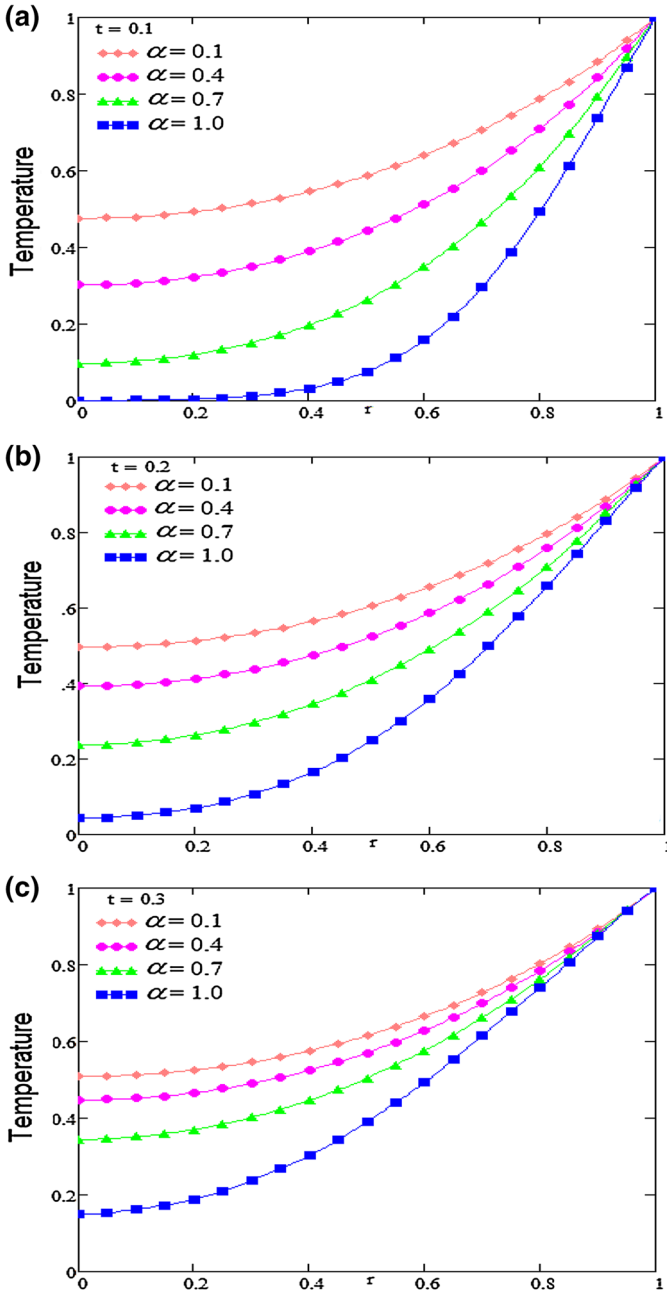


Fig. 2 Profiles of dimensionless temperature versus r , for α variation with $Pr = 3$ and different values of time t

Stehfest’s numerical algorithm. Numerical simulations and graphical illustrations are carried out in order to analyze the influence of the time-fractional derivative on the flow parameters. The significant difference between the fractional fluid flow and ordinary fluid is unraveled.

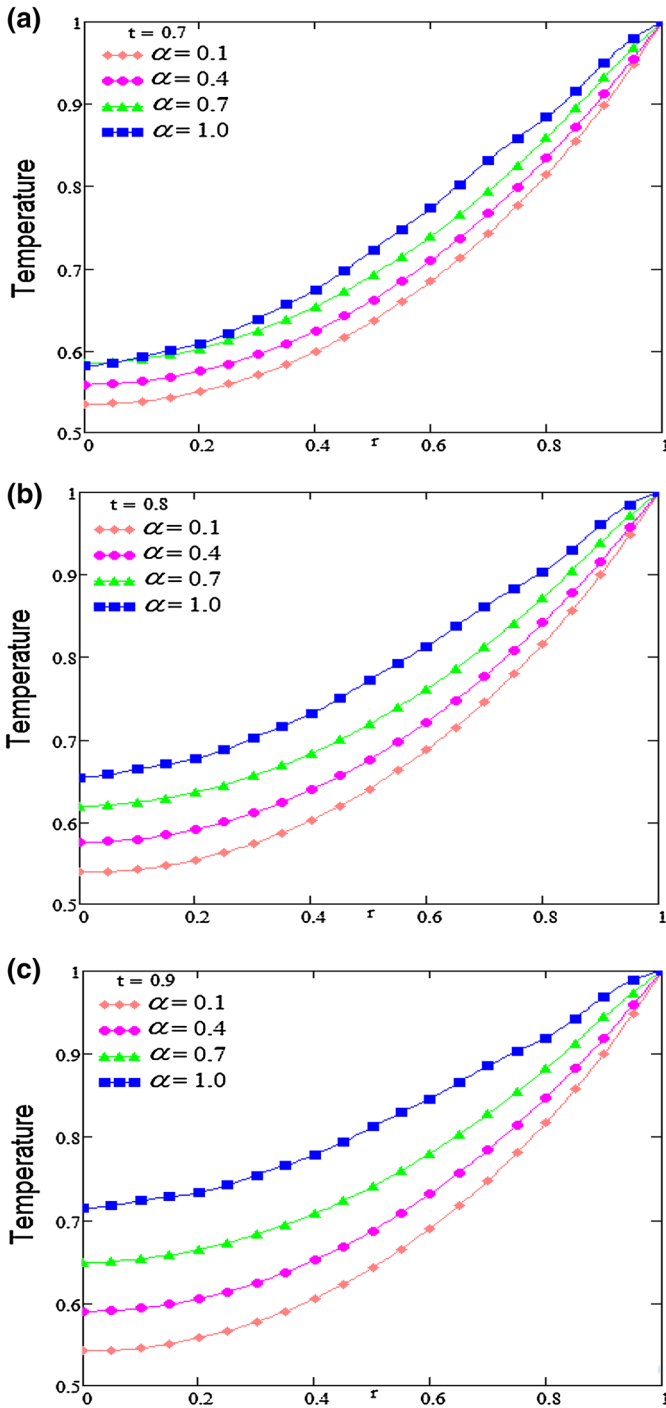


Fig. 3 Profiles of dimensionless temperature versus r , for α variation with $Pr = 3$ and different values of time t

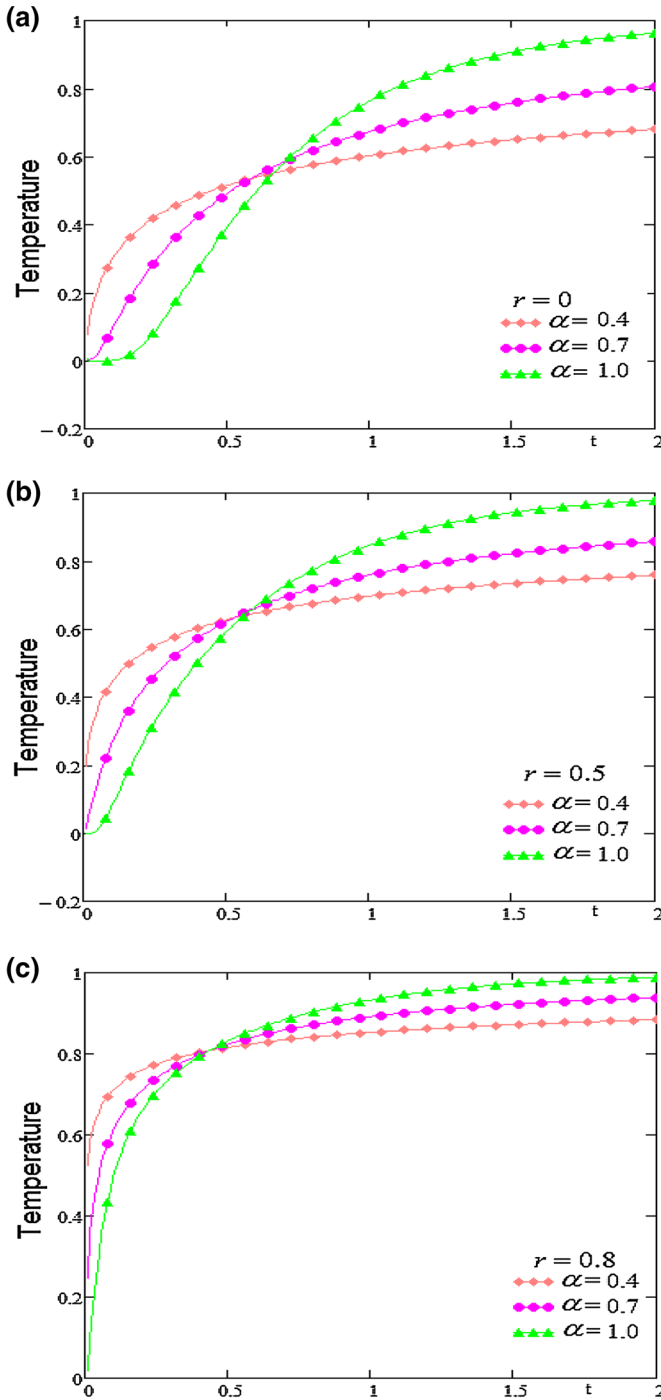


Fig. 4 Profiles of dimensionless temperature versus t , for α variation with $Pr = 3$ and different values of time r

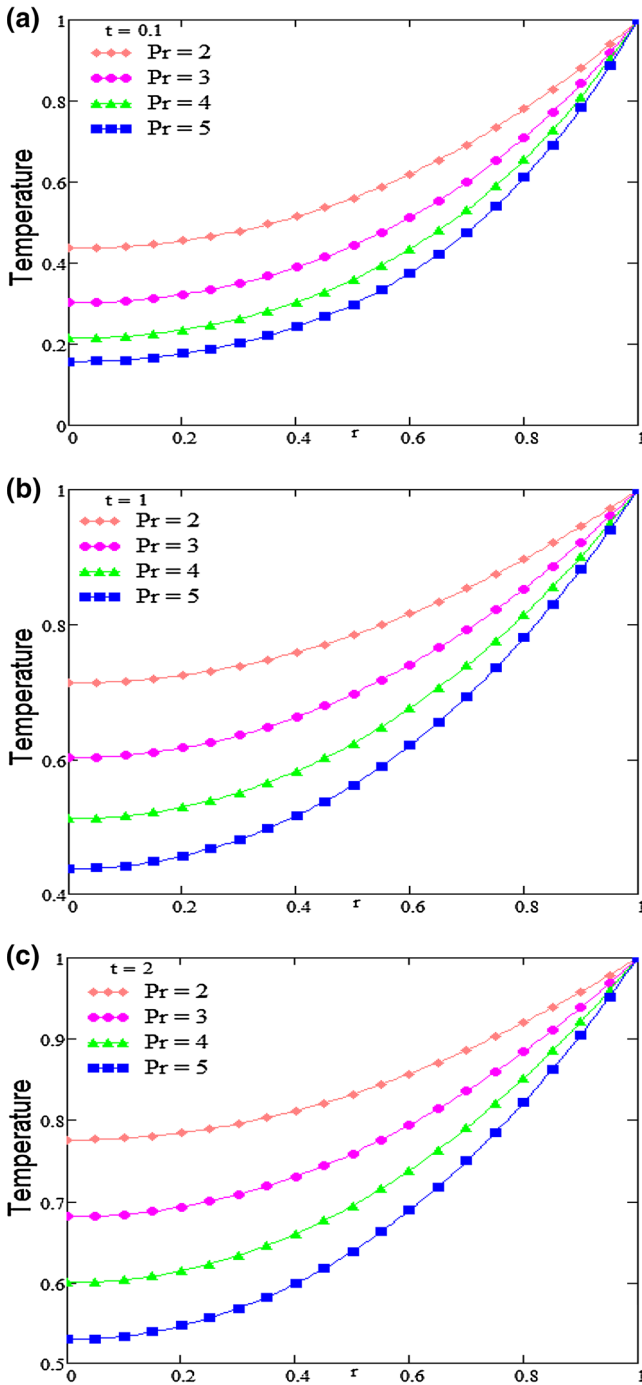


Fig. 5 Profiles of dimensionless temperature versus r , for Pr variation with $\alpha = 0.4$ and different values of time t

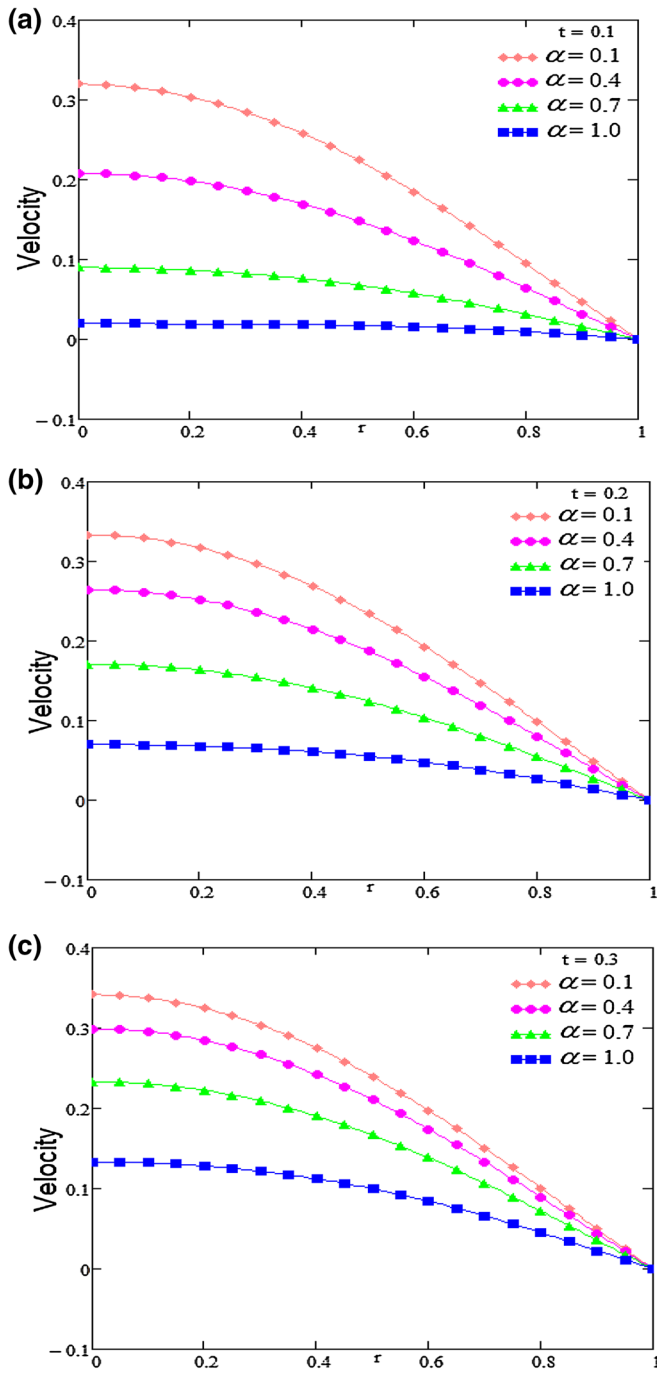


Fig. 6 Profiles of dimensionless velocity versus r , for α variation with $Pr = 2, Sc = 1.5, Gr = 1.5, Gm = 2.5$, and different values of time t

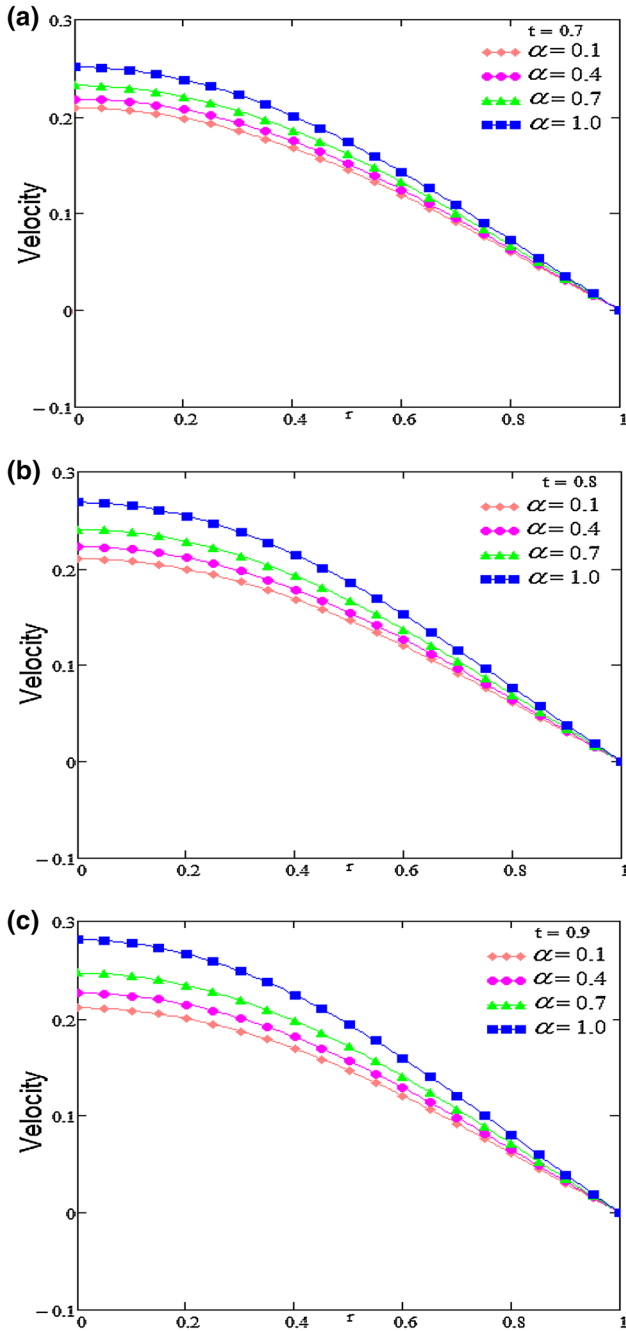


Fig. 7 Profiles of dimensionless velocity versus r , for α variation with $Pr = 2, Sc = 1.5, Gr = 1.5, Gm = 2.5$, and different values of time t

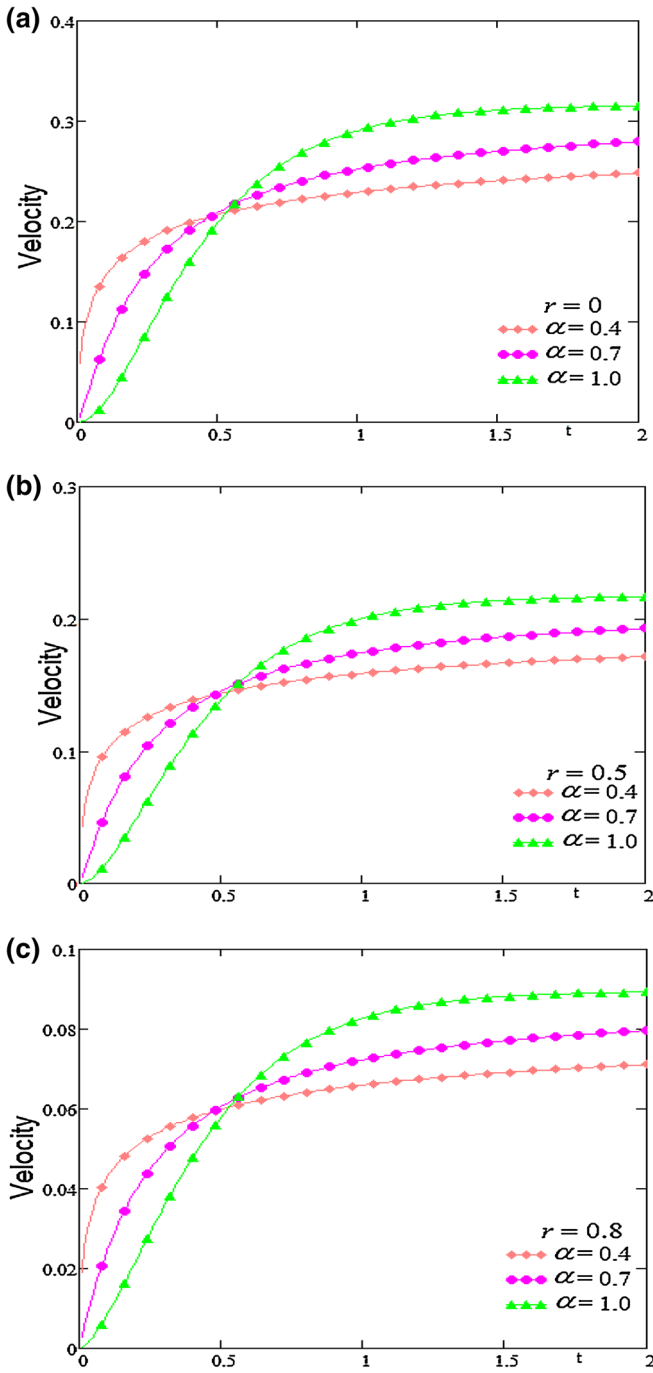


Fig. 8 Profiles of dimensionless velocity versus t , for α variation with $Pr = 2, Sc = 1.5, Gr = 1.5, Gm = 2.5$, and different values of time r

At the initial time, the flow of fractional fluid is faster than the ordinary fluid. The temperature distribution in the flow of fractional fluid ($0.1 \leq \alpha < 1$) at the initial time ($0.1 \leq t \leq 0.3$) is more substantial than that of the ordinary fluid ($\alpha = 1$). Reverse is the case at future values of time $0.7 \leq t \leq 0.9$.

References

- Zhao, J.Q., Abrahamson, J.: The flow in cylindrical cyclones. *Asia Pac. J. Chem. Eng.* **11**(3–4), 201–222 (2003). <https://doi.org/10.1002/apj.5500110403>
- Sharma, A.K., Velusamy, K., Balaji, C.: Conjugate transient natural convection in a cylindrical enclosure with internal volumetric heat generation. *Ann. Nucl. Energy* **35**(8), 1502–1514 (2008). <https://doi.org/10.1016/j.anucene.2008.01.008>
- Franke, M.E., Hutson, K.E.: Effects of corona discharge on free-convection heat transfer inside a vertical hollow cylinder. *J. Heat Transf.* **106**(2), 346–351 (1984). <https://doi.org/10.1115/1.3246679>
- Roschina, N.A., Uvarov, A.V., Osipov, A.I.: Natural convection in an annulus between coaxial horizontal cylinders with internal heat generation. *Int. J. Heat Mass Transf.* **48**(21–22), 4518–4525 (2005). <https://doi.org/10.1016/j.ijheatmasstransfer.2005.05.035>
- Bairi, A.: Transient natural 2D convection in a cylindrical cavity with the upper face cooled by thermoelectric peltier effect following an exponential law. *Appl. Therm. Eng.* **23**(4), 431–447 (2003). [https://doi.org/10.1016/s1359-4311\(02\)00207-7](https://doi.org/10.1016/s1359-4311(02)00207-7)
- Morgan, V.: The overall convective heat transfer from smooth circular cylinders. *Adv. Heat Transf.* **11**, 199–264 (1975). [https://doi.org/10.1016/s0065-2717\(08\)70075-3](https://doi.org/10.1016/s0065-2717(08)70075-3)
- Lemembre, A., Petit, J.P.: Laminar natural convection in a laterally heated and upper cooled vertical cylindrical enclosure. *Int. J. Heat Mass Transf.* **41**(16), 2437–2454 (1998)
- Chen, S.A.H., Humphrey, J.A.C.: Steady, two-dimensional, natural convection in rectangular enclosures with differently heated walls. *J. Heat Transf.* **109**, 400–406 (1987)
- Kim, D.M., Viskanta, R.: Effect of wall heat conduction on natural convection heat transfer in a square enclosure. *J. Heat Transf.* **107**, 139–146 (1985)
- Vargas, M., Sierra, F.Z., Ramos, E., Avramenko, A.A.: Steady natural convection in a cylindrical cavity. *Int. Commun. Heat Mass Transf.* **29**(2), 213–221 (2002)
- Makinde, O.D., Animasaun, I.L.: Bioconvection in MHD nanofluid flow with nonlinear thermal radiation and quartic autocatalysis chemical reaction past an upper surface of a paraboloid of revolution. *Int. J. Therm. Sci.* **109**, 159–171 (2016)
- Makinde, O.D., Animasaun, I.L.: Thermophoresis and Brownian motion effects on MHD bioconvection of nanofluid with nonlinear thermal radiation and quartic chemical reaction past an upper horizontal surface of a paraboloid of revolution. *J. Mol. Liq.* **221**, 733–743 (2016)
- Animasaun, I.L.: 47 nm alumina–water nanofluid flow within boundary layer formed on upper horizontal surface of paraboloid of revolution in the presence of quartic autocatalysis chemical reaction. *Alex. Eng. J.* **55**(3), 2375–2389 (2016)
- Koriko, O.K., Omowaye, A.J., Sandeep, N., Animasaun, I.L.: Analysis of boundary layer formed on an upper horizontal surface of a paraboloid of revolution within nanofluid flow in the presence of thermophoresis and Brownian motion of 29 nm CuO. *Int. J. Mech. Sci.* **124**, 22–36 (2017)
- Kee, R.J., Landram, C.S., Miles, J.C.: Natural convection of a heat generating fluid within closed vertical cylinders and sphere. *J. Heat Transf. Trans. ASME* **98**(1), 55–61 (1976)
- Babu, M.J., Sandeep, N., Saleem, S.: Free convective MHD Cattaneo–Christov flow over three different geometries with thermophoresis and Brownian motion. *Alex. Eng. J.* **56**(4), 659–669 (2017)
- Hayat, T., Makhdoom, S., Awais, M., Saleem, S., Rashidi, M.M.: Axisymmetric Powell–Eyring fluid flow with convective boundary condition: optimal analysis. *Appl. Math. Mech.* **37**(7), 919–928 (2016)
- Nadeem, S., Saleem, S.: An optimized study of mixed convection flow of a rotating Jeffrey nanofluid on a rotating vertical cone. *J. Comput. Theor. Nanosci.* **12**(10), 3028–3035 (2015)
- Nadeem, S., Saleem, S.: Mixed convection flow of Eyring–Powell fluid along a rotating cone. *Res. Phys.* **4**, 54–62 (2014)
- Nadeem, S., Saleem, S.: Analytical treatment of unsteady mixed convection MHD flow on a rotating cone in a rotating frame. *J. Taiwan Inst. Chem. Eng.* **44**(4), 596–604 (2013)
- Animasaun, I.L.: Double diffusive unsteady convective micropolar flow past a vertical porous plate moving through binary mixture using modified Boussinesq approximation. *Ain Shams Eng. J.* **7**, 755–765 (2016). <https://doi.org/10.1016/j.asej.2015.06.010>

22. Animasaun, I.L.: Dynamics of unsteady MHD convective flow with thermophoresis of particles and variable thermo-physical properties past a vertical surface moving through binary mixture. *Open J. Fluid Dyn.* **5**, 106–120 (2015). <https://doi.org/10.4236/ojfd.2015.52013>
23. Animasaun, I.L.: Effects of thermophoresis, variable viscosity and thermal conductivity on free convective heat and mass transfer of non-darcian MHD dissipative Casson fluid flow with suction and n th order of chemical reaction. *J. Niger. Math. Soc.* **34**, 11–31 (2015). <https://doi.org/10.1016/j.jnms.2014.10.008>
24. Bohn, M.S., Anderson, R.: Temperature and heat flux distribution in a natural convection enclosure flow. *J. Heat Transf. Trans. ASME* **108**, 471–476 (1986)
25. Liaqat, A., Baytas, A.C.: Conjugate natural convection in a square enclosure containing volumetric sources. *Int. J. Heat Mass Transf.* **44**(17), 3273–3280 (2001)
26. Kuznetsov, G.V., Sheremet, M.A.: Conjugate heat transfer in an enclosure under the condition of internal mass transfer and in the presence of the local heat source. *Int. J. Heat Mass Transf.* **52**, 1–8 (2009)
27. Sasso, M., Palmieri, G., Amodio, D.: Application of fractional derivative models in linear viscoelastic problems. *Mech. Time Depend. Mater.* **15**(4), 367–387 (2011)
28. Sloninsky, G.L.: Laws of mechanical relaxation processes in polymers. *J. Polym. Sci.* **16**, 1667–1672 (1967)
29. Bagley, R.L., Torvik, P.J.: A theoretical basis for the application of fractional calculus to viscoelasticity. *J. Rheol.* **27**, 201–210 (1983)
30. Schiessel, H., Blumen, A.: Hierarchical analogues to fractional relaxation equations. *J. Phys. Math. Gen.* **26**, 5057–5069 (1993)
31. Song, D.Y., Jiang, T.Q.: Study on the constitutive equation with fractional derivative for the viscoelastic fluids—modified Jeffreys model and its application. *Rheol. Acta* **37**, 512–517 (1998)
32. Djordjevic, V.D., Jaric, J., Fabry, B., Fredberg, J.J., Stamenovic, D.: Fractional derivatives embody essential features of cell rheological behavior. *Ann. Biomed. Eng.* **31**, 692–699 (2003)
33. Heymans, N.: Fractional calculus description of non-linear viscoelastic behavior of polymers. *Nonlinear Dyn.* **38**, 221–231 (2004)
34. Liu, H., Oliphant, T.E., Taylor L.: General fractional derivative viscoelastic models applied to vibration elastography. In: *Proceedings of IEEE Ultrason Symposium*, pp. 933–936 (2003)
35. Chatterjee, A.: Statistical origins of fractional derivatives in viscoelasticity. *J. Sound Vib.* **284**, 1239–1245 (2005)
36. Pfitzenreiter, T.: A physical basis for fractional derivatives in constitutive equations. *Z. Angew. Math. Mech.* **84**, 284–287 (2004)
37. Kawada, Y., Nagahama, H., Hara, H.: Irreversible thermodynamic and viscoelastic model for power-law relaxation and attenuation of rocks. *Tectonophysics* **427**, 255–263 (2006)
38. Deka, R.K., Paul, A., Chaliha, A.: Transient free convection flow past vertical cylinder with constant heat flux and mass transfer. *Ain Shams Eng. J.* **8**(4), 643–651 (2015). <https://doi.org/10.1016/j.asej.2015.10.006>
39. Lorenzo, C.F., Hartley, T.T.: Generalized functions for the fractional calculus. *Crit. Rev. Biomed. Eng.* **36**(1), 39–55 (2008). <https://doi.org/10.1007/bfb0067108>
40. Stehfest, H.: Algorithm 368. Numerical inversion of Laplace transforms. *Commun. ACM* **13**(1), 47–50 (1970)
41. Fu, Z.J., Chen, W., Yang, H.T.: Boundary particle method for Laplace transformed time fractional diffusion equations. *J. Comput. Phys.* **235**, 52–66 (2013). <https://doi.org/10.1016/j.jcp.2012.10.018>
42. Fu, Z.J., Chen, W., Qin, Q.H.: Three boundary meshless methods for heat conduction analysis in nonlinear FGMs with Kirchhoff and Laplace transformation. *Adv. Appl. Math. Mech.* **4**(5), 519–542 (2012). <https://doi.org/10.4208/aamm.10-m1170>